

A new electric streamer for the characterization of river embankments

Original

A new electric streamer for the characterization of river embankments / Comina, C., Vagnon, F., Arato, A., Fantini, F., Naldi, M.. - In: ENGINEERING GEOLOGY. - ISSN 0013-7952. - 276:105770(2020), pp. 1-10.
[10.1016/j.enggeo.2020.105770]

Availability:

This version is available at: 11583/2957377 since: 2022-03-05T09:14:30Z

Publisher:

Elsevier BV

Published

DOI:10.1016/j.enggeo.2020.105770

Terms of use:

This article is made available under terms and conditions as specified in the corresponding bibliographic description in the repository

Publisher copyright

Elsevier preprint/submitted version

Preprint (submitted version) of an article published in ENGINEERING GEOLOGY © 2020,
<http://doi.org/10.1016/j.enggeo.2020.105770>

(Article begins on next page)

1 **A new electric streamer for the characterization of river**
2 **embankments.**

3
4 Comina C.¹, Vagnon F.¹, Arato A., Fantini F., Naldi M.²
5 ¹Dipartimento di Scienze della Terra, Università degli studi di Torino, Torino (IT)
6 ² Techgea S.r.l., Torino (IT).

7
8
9
10 **ABSTRACT**

11 River embankments are linearly extended earth structures, worldwide diffused, built for river flood
12 protection. Their integrity and stability are fundamental prerequisites for the protection efficiency
13 they can offer, also in relation to the increasing frequency and magnitude of extreme flood events due
14 to climate changes. Proper characterization and monitoring of the embankments' body are essential
15 to verify the construction requirements of newly built structures and to evaluate the durability of aged
16 ones. Given their significant linear extension, the characterization cannot rely only on local
17 geotechnical investigations but requires the application of efficient and economically affordable
18 methods, able to investigate relevant lengths in a profitable way. This is even more essential when
19 the investigations are performed after, or in foresee of, significant flood events, when embankment
20 structures get stressed and timing of the surveys is crucial. In these conditions, new survey
21 methodologies, eventually with the use of mobile systems, are a main research topic. In this paper the
22 application of a new electric streamer, specifically designed for these aims, is presented. The technical
23 solutions adopted for its construction are described and its application to the characterization of three
24 different river embankments is presented. The case studies were chosen in accordance with the Po
25 River Interregional Agency (AIPO), which is the authority deputed to the management of
26 hydrographic network of Po River and to the safety of protection structures against flood risk in
27 North-West Italy. The selected embankments are all earth type structures, constructed above the
28 natural alluvial soils, but are characterized by different conditions and problematics. The results
29 obtained with the new system are comparable to standard Electric Resistivity Tomography (ERT)
30 methods. The newly developed system has however significant advantages in terms of reducing the
31 survey time, improving the efficiency of the surveys and increasing the data coverage for a better
32 definition of potentially dangerous anomalies.

33
34
35
36

37 **Article Highlights:**

- 38 • A new electric streamer has been developed for the characterization of river embankments;
39 • Application of the new electric streamer produces results comparable to those from standard
40 geoelectrical surveys (ERT);
41 • Advantages in survey time and efficiency are highlighted.

42 **Keywords:** Electric streamer, ERT, river embankments.

43 **Corresponding author:** Cesare Comina, cesare.comina@unito.it

45 1. INTRODUCTION

46 River embankments are linearly extended earth structures constructed to serve as flood control
47 systems during large rain events. A proper characterization of the embankment body is essential both
48 after its construction, or partial rebuilding interventions, to verify uniformity and correspondence to
49 design characteristics, and during its operating life, to monitor integrity losses caused by natural
50 events or wildlife activities (e.g. animal burrows). Floods, seepages and invasive animal activities are
51 indeed known to negatively affect the hydraulic performances of embankments, and their structural
52 integrity. Maintenance and control of embankments integrity is specifically of fundamental
53 importance following, or during, main flood events which could severely compromise the efficiency
54 of specific embankment portions. In recent years, frequency and magnitude of extreme flood events
55 have been rapidly increasing in Central America, Southern Europe and in Italy because of climate
56 changes. Moreover, the poor maintenance of hydraulic structures, mostly reaching their design
57 service life, makes the adoption of specific interventions of paramount international relevance.

58 Given the significant length of these structures, their characterization cannot rely only on local
59 geotechnical investigations but requires the application of efficient and economically affordable
60 methods, able to investigate the whole embankments in a profitable way. With this respect, non-
61 invasive, rapid and cost-effective methods are desirable to identify higher potential hazard zones for
62 planning detailed interventions and target rehabilitation efforts. The speed of the surveys is an
63 important prerequisite when interventions must be planned in a reduced time window close to main
64 events and when a first draft characterization of the state of life of the embankments is required.

65 Geophysical methods, and predominantly geoelectrical ones, are particularly suitable for these aims
66 since they can cover long survey lengths with reduced economic and time effort. Geoelectrical
67 measurements can investigate variations of soil composition and water saturation, detect development
68 of weak zones and identify local anomalies potentially related to wildlife activity (e.g. burrows). In
69 the scientific literature, several application of electrical resistivity tomography (ERT) to river
70 embankments and earth dams have been shown in order to: locate fissures and desiccation cracks
71 (e.g. [Jones et al., 2014](#); [An et al., 2020](#)), detect animal burrows (e.g. [Borgatti et al., 2017](#)), detect
72 seepages and leakage problems (e.g. [Panthulu et al., 2001](#); [Cho and Yeom, 2007](#); [Al-Fares, 2014](#);
73 [Busato et al., 2016](#); [Lee et al., 2020](#)), monitor water saturation (e.g. [Arosio et al., 2017](#); [Tresoldi et](#)
74 [al., 2019](#); [Jodry et al., 2019](#)), ascertain geometrical characteristics and internal properties to serve as
75 guidance for the rehabilitation interventions (e.g. [Cardarelli et al., 2014](#); [Minsley et al., 2011](#); [Sjödahl](#)
76 [et al., 2006](#); [Camarero et al., 2019](#)) and in general for vulnerability assessment.

77 ERT cannot be considered as a stand-alone technique since electrical resistivity depends on both
78 electrolytic conduction (fluid saturation and ionic composition) and interfacial/surface conduction

79 (presence of clayey particles or organic matter). The entity of the two contribution is not easily
80 distinguishable from survey results. Electrical resistivity is a complex quantity, composed by an in-
81 phase component related to electrolytic conduction, and an out-of-phase component, mainly
82 associated to Induced Polarisation (IP) mechanisms belonging to interfacial conduction from soil
83 surface charge (Cation Exchange Capacity). These two different phenomena can be measured either
84 in frequency domain or in time domain. Spectral Induced Polarization (SIP) implies the collection of
85 module and phase of complex resistivity in frequency domain, spanning over a frequency range
86 usually from 0.1 Hz up to 1 kHz (e.g., Borner et al., 1996, Binley et al., 2005). In time domain,
87 electrical resistivity is obtained by direct current (DC) potential parameters, while the polarization
88 mechanisms are estimated by the chargeability parameter, defined as the integral of a residual voltage
89 decay after current switch-off.

90 Several applications of this IP methodology to the characterization of dams and river embankments
91 can be found in literature (e.g. [Abdulsamad et al., 2019](#); [Soueid et al., 2020a](#)). Nevertheless, ERT is
92 still often adopted as a first characterization tool since the execution of ERT surveys is significantly
93 less time consuming than IP ones. Therefore, when the time of the surveys is a requirement, ERT is
94 the most often chosen method.

95 The main aim of this paper is to evaluate whether the standard ERT surveys could be further
96 improved, mainly in terms of reducing surveying time, for increasing the investigation distance along
97 the embankments in a single day of acquisition. Since the generation of resistivity pseudo-sections
98 from ERT surveys is a standardized step, faster surveys could also allow for a quasi-real time
99 processing, mapping the resistivity distribution along the investigated embankments with the
100 advantage of directly identifying potentially dangerous anomalies and planning more extensive
101 surveys.

102 Improvement of the efficiency and feasibility of ERT surveys can potentially rely on the use of mobile
103 systems dragging the appropriate instrumentation, disposed along a streamer, behind a vehicle. This
104 alternative survey strategy can potentially avoid the long operation of nailing electrodes in the ground
105 and speeding the acquisition time.

106 Some systems based on this approach were developed in the past by using capacitive coupled methods
107 with electromagnetic antennas, at operating frequencies in the quasi static field, carried on the surface
108 (e.g. CCR (Capacitive Coupled Resistivity), OhmMapper from Geometrics and CRI (Capacitive
109 Resistivity Imaging), [Kuras et al., 2007](#)). However, in low resistivity soils, such as clays or saturated
110 silts, commonly used to build river embankments, hydraulic barriers and earth dams, capacitively
111 coupled systems may encounter limitations in current injection within the ground. This is mainly
112 originated by the electromagnetic interference between the antennae and the low resistivity

113 underground that leads to a shallow distribution of the induced current flow in the subsoil. The skin
114 depth is then limited and signal-to-noise ratio decreases, resulting in low quality data, particularly for
115 large antennas separation (i.e. greater investigation depths) and when the contact between antennas
116 and the ground is not properly controlled (Lee et al., 2002).

117 For these reasons, the most recent development of mobile geoelectric systems has been redirected
118 towards a recovery of the galvanic coupling approach. An example of this is the ARP (Automatic
119 Resistivity Profiling, from Geocharta) system, which involves the use of wheel-based electrodes
120 inserted in the ground and rolled along the surface. However, this system adopts reduced electrode
121 separation and the investigation depth is consequently limited, making it suitable for precision
122 agricultural investigations (e.g. Dabas, 2011). One of the older systems involving the use of electrodes
123 with increased separation distances dragged behind a vehicle is the PACEP (Pulled Array Continuous
124 Electrical Profiling, Sorensen, 1996). The latter system is based on a more versatile electrode
125 disposition, and hence the achievable survey depths can be accordingly increased.

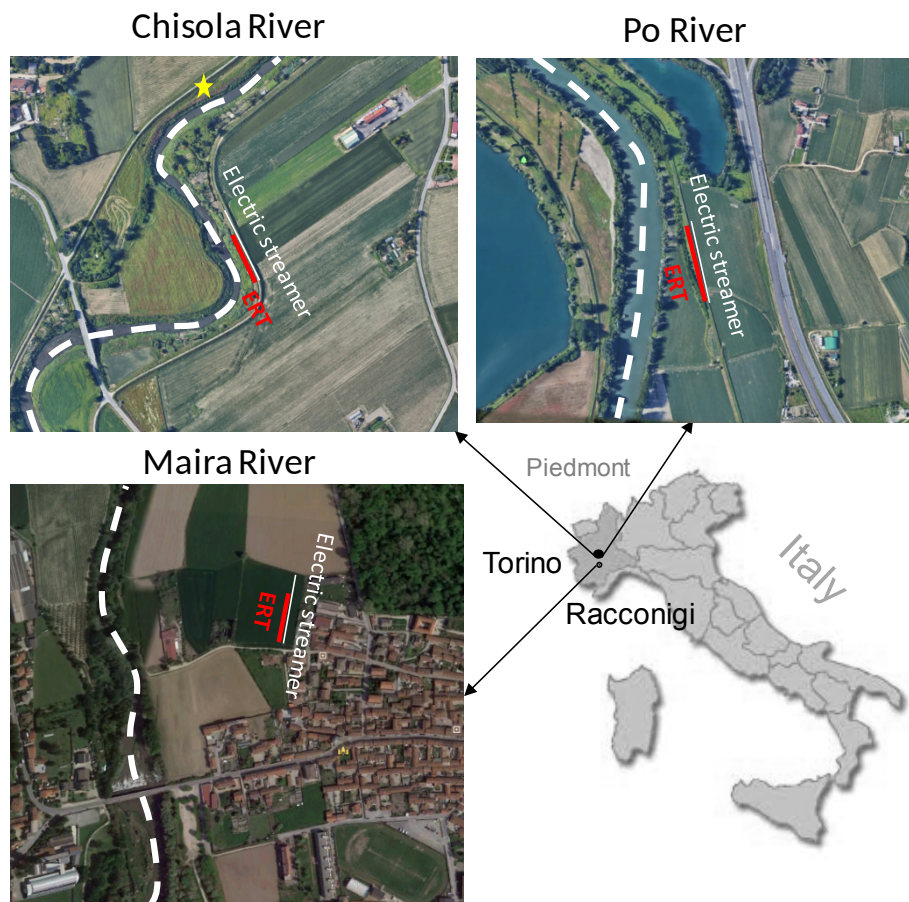
126 This last system has been of inspiration for the development of a newly conceived geoelectrical
127 streamer, also based on galvanic coupling approach but with brand new electrode design and
128 technological details. The main research aims in developing this new streamer were related to: i)
129 allow the execution of fast geoelectric surveys in motion along river embankments and, in general,
130 linearly extended earth structures; ii) guarantee an investigation depth covering the whole
131 embankment and foundation soil, overcoming current limitations of available similar instrumentation
132 usually adopted for geoelectrical surveys in motion; iii) potentially allow for a quasi-real time
133 imaging of the pseudo-section during surveys execution for a preliminary screening of the
134 embankments; iv) develop a system that could be ideally combined with standard seismic streamers.
135 An appropriate disposition of the electrodes along the streamer, and the use of different measurement
136 combinations, allowed to set-up a measuring system for ERT in motion with similar, or even
137 increased, resolution compared to standard ERT surveys. This innovative measuring approach is an
138 improvement with respect to available methods for the execution of geoelectrical surveys in motion
139 and present peculiar advantages in terms of speed of the surveys and direct imaging of potential
140 anomalies. The newly developed instrumentation is presented in this paper, and the results obtained
141 from test surveys in three different case studies are compared to standard ERT acquisitions to
142 demonstrate its effectiveness.

143

144 2. CASE STUDIES

145 The presented case studies were defined in accordance with the River Po Interregional Agency
146 (AIPO), which is the authority deputed to the management of hydrographic network of the Po river,

147 the main river crossing northern Italy from West to East. Particularly, AIPO has focused its interest
 148 in three different embankment portions in the surrounding of the cities of Torino and Racconigi, in
 149 Piedmont region (Figure 1). The attention of AIPO has raised in recent years following main flood
 150 events (the most recent one in November 2019) which have affected several embankments portions
 151 and inundated the surrounding countryside and portions of some cities. The selected embankments
 152 are all earthen structures, constructed above the natural alluvial soils of the plain (mostly sand and
 153 gravels), but are characterized by different conditions and problematics.



154
 155 **Figure 1 – Location of the case studies in the north western Italian Po plain, Piedmont region, and detail**
 156 **of the studied embankments and executed surveys.**

157 The Maira river embankment is a shallow (about 1.5 m height) newly constructed embankment which
 158 protects the borders of the city of Racconigi. This embankment was constructed with selected uniform
 159 clayey material. Here, AIPO is interested in assessing the global uniformity inside the embankment
 160 and to evaluate the effectiveness of its construction, following the occurrence of some lateral landslips
 161 along the slopes, caused by the transit of heavy trucks and excavators. The Chisola river embankment
 162 is a 2.5 m high mostly silty (98.5 % passing to the 0.4 mm sieve) embankment. It is considered critical
 163 due to its peculiar location near river meanders, which significantly increase river erosion potential
 164 during flood events. Indeed, in a similar bend, north from the present survey location, a rupture of the

165 left embankment was recently noted following the flood events of November 2016 (yellow star in
166 [Figure 1](#)). Repair works are ongoing in the already affected portion, but attention is related to eventual
167 extension of the interventions also to the studied embankment side. Along these two embankments a
168 thin gravel layer was put in place to pave the road on the embankment summit. Finally, the Po river
169 embankment is 2 m high and serves as protection to the main highway from Torino towards the south.
170 It is the eldest among the three embankments, built in early 20th century using natural material (sands
171 and gravels) probably exploited from surrounding caves or directly from river deposits. Along this
172 embankment, several badger burrows were observed.

173 The interest of AIPO is related to the potential of the newly developed electric streamer in providing
174 a fast and cost-effective identification of resistivity anomalies related to the different problematics
175 evidenced in the case studies. Investigations along the three river embankments were therefore
176 planned. The first aim of the surveys is a comparison between data obtainable with standard ERT
177 measurements and the newly developed system; with this aim, both techniques were applied over
178 superimposing portions along the studied embankments ([Figure 1](#)). Following this comparison, the
179 interpretation of the evidenced anomalies is also provided to help the management authority in
180 monitoring the integrity of the studied embankments portions.

181

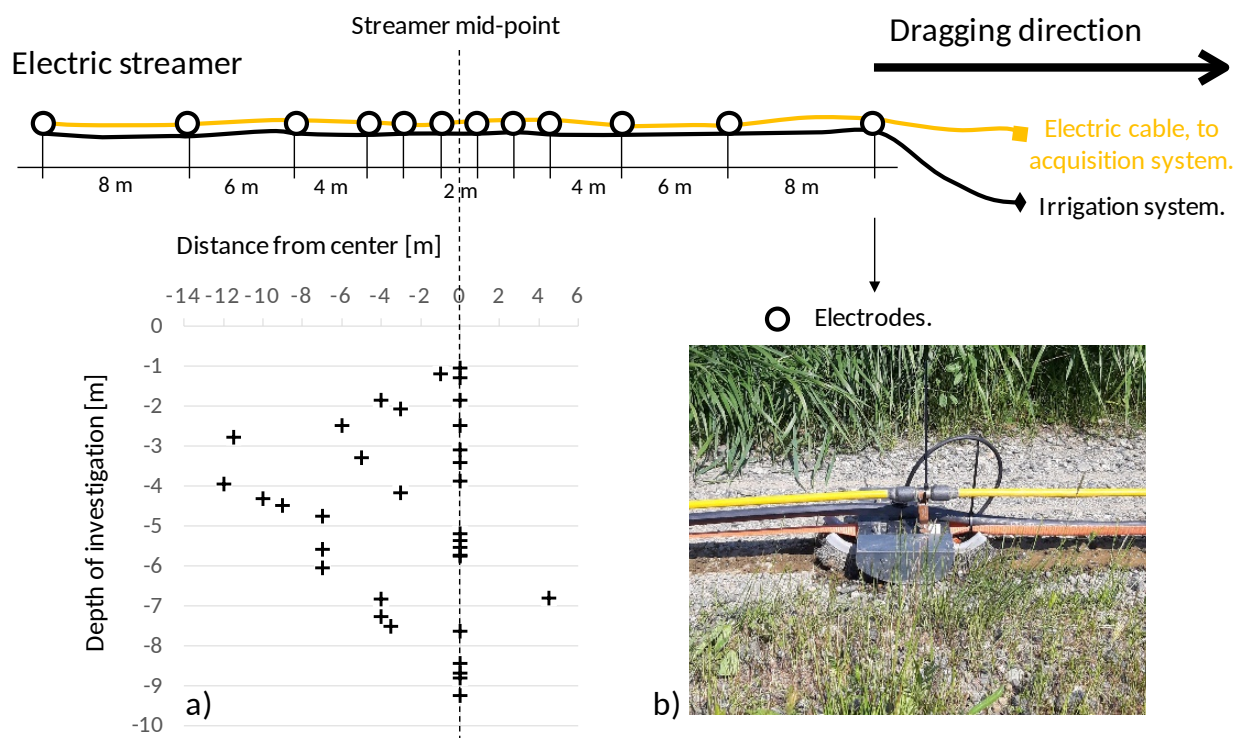
182 **3. ELECTRIC STREAMER AND EXECUTED SURVEYS**

183 Electrical resistivity measurements involve the use of 4 electrodes (measurement quadrupole). Two
184 of them (current electrodes) inject into the ground the desired current amount (I), while the other two
185 (potential electrodes) measure the resulting potential difference (V). From these two measured values
186 the apparent resistivity (ρ_a) of the subsoil can be obtained through:

$$187 \quad \rho_a = k \frac{V}{I} \quad (1)$$

188 where k is a geometric factor that, for a half-space with electrodes at the interface, depends on the
189 electrodes arrangement within the quadrupole and is computable according to standard quadrupole
190 dispositions (e.g. Wenner-Schlumberger and Dipole-Dipole). Generally, k depends also from
191 topography and boundary conditions and can be computed numerically for any geometry, solving
192 Laplace equation with finite element methods (e.g. [Jougnot et al., 2010](#)). The apparent resistivity is
193 therefore the raw experimental result obtainable with the acquisitions. Depending on the disposition
194 and distance of the electrodes, each measured apparent resistivity value can be related to different
195 portions of the subsoil: increased electrode separations involve deeper current fluxes and therefore

196 greater investigation depths; lateral resistivity variations can be detected by moving the quadrupole
 197 horizontally along the survey profile.
 198 If the comparison of the apparent resistivity distribution obtained with different measuring
 199 approaches gives similar outcomes, this can be considered as a direct indicator of the quality and
 200 reliability of the adopted alternative measuring methods. Apparent resistivity values acquired with
 201 the new electric streamer and with standard galvanometric ERT approach will be therefore compared
 202 in this work, using standard ERT data as comparison benchmark, to prove the validity and
 203 applicability of proposed acquisition system.
 204 Reconstructing the real resistivity distribution of the subsoil from apparent resistivity measurements
 205 involves the solution of an inverse problem. This can be performed in tomographic approach if the
 206 raw data distribution offers enough spatial coverage. Quality of the reconstructed resistivity
 207 distribution depends on quality and spatial distribution of the raw data. The two acquisition systems
 208 involve different data distributions along the survey length (see later). Inverted resistivity data from
 209 the new electric streamer and standard ERT approach will be therefore compared in this work to
 210 establish if the reconstructed resistivity distribution contain the same relevant information for the
 211 investigated embankments.
 212 A scheme of the electric streamer designed for the execution of resistivity measurements in motion
 213 is displayed in [Figure 2](#).



214 **Figure 2 – Scheme of the electric streamer adopted for the surveys, in a) the depth of investigation of**
 215 **the different acquired measurements is reported, in b) the detail of a single electrode is depicted with**
 216 **evidence of the irrigation system (black) and of the multipolar cable (yellow).**
 217

218 The streamer foresees the use of specifically designed electrodes and an appropriate drip irrigation
219 system (Figure 2b). Combining these two technical solutions allows to reduce contact resistances
220 between the electrodes and the ground. Electrodes were constructed in stainless steel and have the
221 form of brushes, i.e. containing several thin wires, in order to increase the contact surface to the
222 ground and further reduce electric contact resistances. The shape of the brushes is similar to a sled to
223 allow for an easy dragging of the streamer. On top of these brushes a PVC element is also present
224 with lateral wings leaning to the ground in order to avoid overturning during dragging. Preliminary
225 calibration tests, for single quadrupoles acquisitions, have evidenced that data acquired with this
226 system are comparable to standard geoelectrical surveys (Arato et al., 2020). Particularly, several
227 comparisons of dripped and dry contact resistances were performed. A strong reduction (around 75%
228 on average) of contact resistances after dripping was observed, highlighting the importance of the
229 irrigation system for this survey. The arrangement of the electrodes along the streamer is very
230 versatile and can be adapted according to different investigation requirements.

231 In the configuration used in this study the streamer has a length of 46 m and 12 active electrodes, that
232 can be used both as current and potential electrodes, placed at progressively increasing spacings,
233 symmetrically centred around the streamer mid-point (Figure 2). The nearest electrodes are the ones
234 aside the streamer mid-point (6 electrodes at 2 m separation) while the farthest ones are at the
235 extremes of the streamer (8 m separation). The adopted disposition allows to perform different
236 measurement combinations, with different vertical and horizontal positions. Given that survey depth
237 is directly proportional to electrodes separation, shallow information is obtained from the
238 measurements performed with the nearest electrodes and deeper information from measurements
239 performed with the electrodes at the cable extremes. The measuring sequence here adopted is based
240 both on the Wenner-Schlumberger (26 measurements) and Dipole-Dipole (8 measurements)
241 quadrupoles and guarantees an adequate data coverage from the surface to an estimated depth of about
242 10 meters (Figure 2a). The depth of investigation of each quadrupole was assumed with reference to
243 the pseudo-depth formulated by Res2DInv software (Loke and Barker, 1996) given each electrodes
244 disposition. The pseudo-depth is the median depth of investigation, computed from the sensitivity
245 curve and defined as the depth value at which the integral under the sensitivity curve is equally
246 divided (e.g. Edwards, 1977, Barker, 1989).

247 With the adopted sequence most of the measuring points are located along the vertical below the
248 streamer mid-point (replicating a sort of vertical electric sounding); off-vertical measurements are
249 used to increase the lateral coverage and depth levels not covered by the quadrupoles below the
250 streamer mid-point. Repeating the measuring sequence for different positions of the streamer mid-
251 point (measurement step), it is therefore possible to build an apparent resistivity pseudo-section that

252 can be subsequently elaborated with tomographic methods. A measurement step equal to 2 m was
 253 adopted in all the surveys here reported. For the different case studies the resulting survey length and
 254 number of electric streamer measurements is reported in [Table 1](#). The survey length refers to the
 255 distance between the first streamer mid-point to the last. However, as it can be observed from [Figure](#)
 256 [2a](#), the effective survey length is partially increased by the presence of measurements located also
 257 before the first streamer mid-point.

258 The streamer is dragged, for each measurement step, by a vehicle that stores the equipment necessary
 259 for performing the resistivity measurements (acquisition system and water tank). The electrodes are
 260 connected to the acquisition system (Syscal-Pro, Iris Instruments, georesistivimeter) by means of a
 261 multipolar cable ([Figure 2b](#)).

262

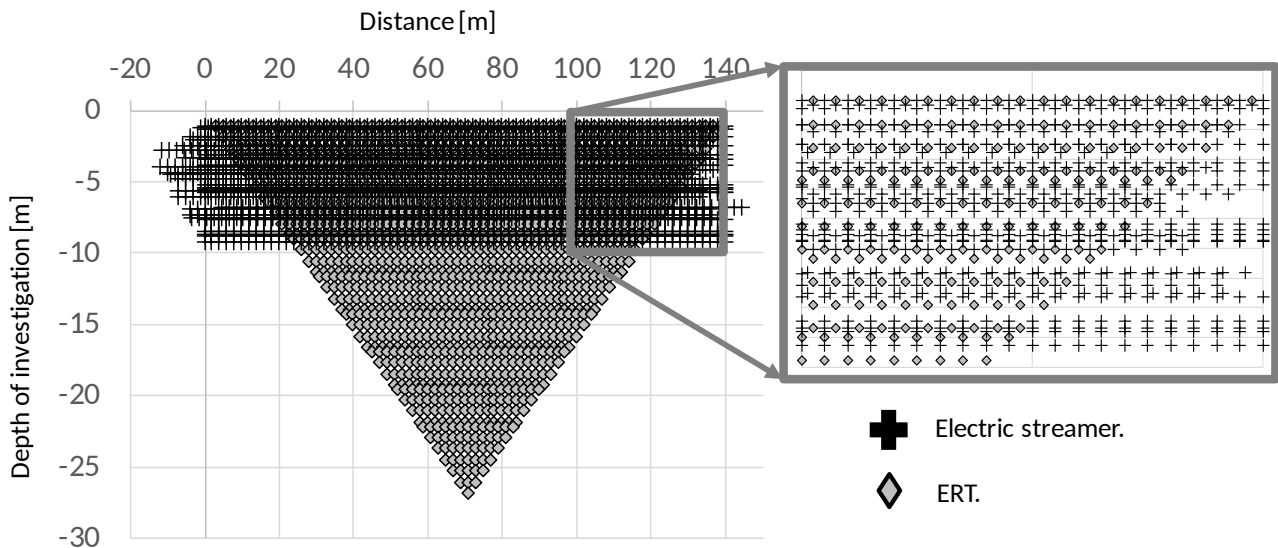
263 **Table 1 – Detail of the executed surveys along the studied embankments. For ERT, both the total number**
 264 **of measurements and the number of measurements covering the first 10 m depth are reported.**

	Survey length [m]		Number of measurements	
	ERT	Electric Streamer	ERT	Electric Streamer
Maira River	94	84	565 (437 within 10 m)	1428
Chisola River	94	120	565 (437 within 10 m)	2074
Po River	142	142	1377 (802 within 10 m)	2448

265

266 For comparison and calibration purposes, standard ERT measurements were also executed along the
 267 portions of the investigated embankments ([Figure 1](#)). These latter were acquired with the same
 268 acquisition system adopted for the electric streamer and 72 (for the Po river case history) or 48 (for
 269 Maira and Chisola rivers case histories) nailed electrodes at 2 m spacing ([Table 1](#)). Standard ERT
 270 data were acquired with a the Wenner-Schlumberger array. For the different survey lengths involved
 271 in the case studies, the resulting number of ERT measurements is reported in [Table 1](#). The resulting
 272 number of measurements levels and total measurements is in the range of commonly adopted values
 273 for ERT investigations. For both the streamer and ERT, measurements were conducted with a 3-cycle
 274 reversing square wave with a 250 ms current on time. This allowed also the determination of
 275 instrumental standard deviation.

276 An example of the data coverage obtainable with the two acquisition systems along the longest of the
 277 executed surveys (Po river) is reported in [Figure 3](#).



278

279 **Figure 3 – Data coverage obtained with the two acquisition systems along the Po river case study.**

280 Data distribution reported in [Figure 3](#) highlights the greater depth of investigation offered by the
 281 standard ERT survey, given the investigated length, due to the increased electrodes separation along
 282 the whole survey line. However, within the depth range of interest in this study, and generally for the
 283 characterization of embankments body and shallow foundation soils (i.e. within the first 10 m), the
 284 streamer data coverage is improved, both laterally and vertically, in comparison to the standard ERT
 285 acquisition sequence adopted. Within this investigation depth the number of data acquired with the
 286 electric streamer is more than three times the ones of ERT (see also [Table 1](#)).

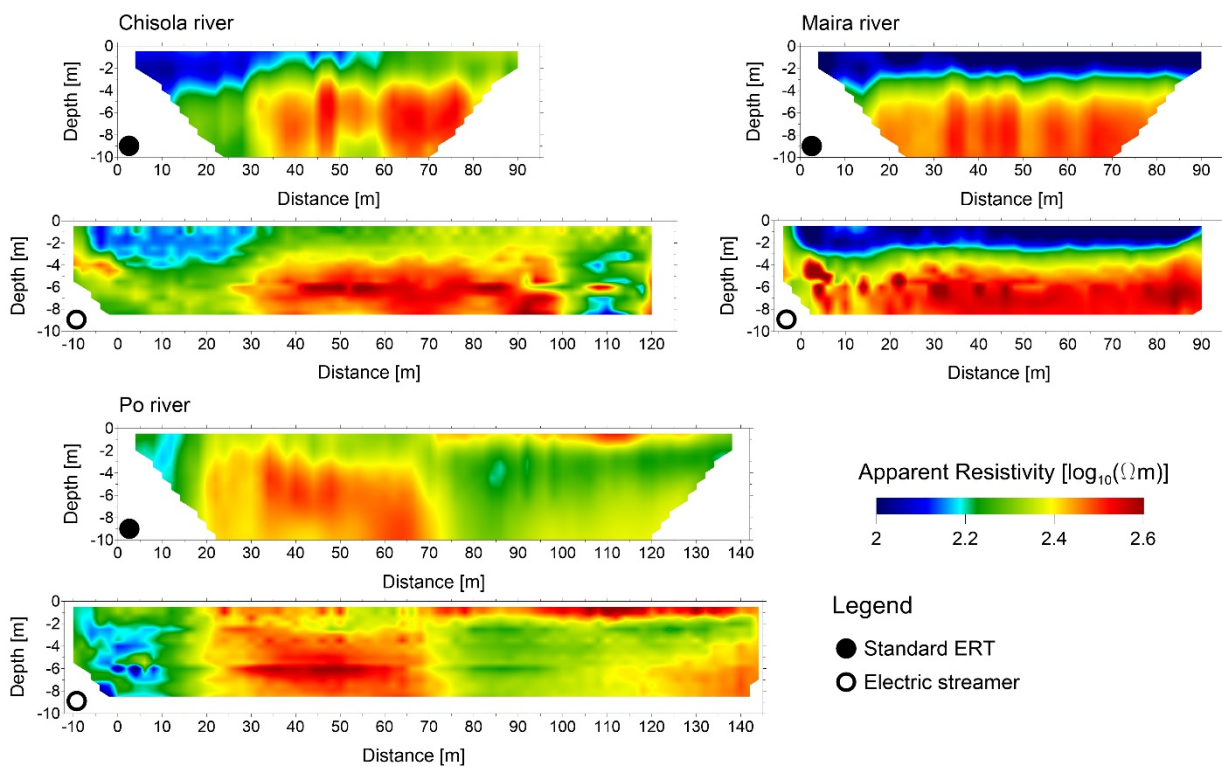
287 Highly noisy data acquired in the two survey modes were preliminary removed adopting several
 288 filtering criteria: i) measurements with an instrumental standard deviation greater than 2%; ii)
 289 quadrupoles belonging to badly ground-coupled electrodes; iii) quadrupoles with transmitted currents
 290 lower than 0.1 mA; iv) apparent resistivity values higher than a certain threshold, established on the
 291 average of measurements. Following the above criteria some of the Dipole-Dipole measurements
 292 acquired with the electric streamer were removed due to their low quality. Lastly, singular outliers
 293 identified by visual analysis of the apparent resistivity profiles and pseudo-sections were also
 294 removed. Filtered data were interpolated along the studied embankments to allow for a 2D
 295 visualization of the apparent resistivity distributions from both surveys. This interpolation was
 296 performed in Surfer (Golden software) with an interpolation grid of 2 m in the horizontal direction
 297 (equal to the acquisition step) and of 0.25 m in the vertical direction. Apparent resistivity data were
 298 then processed and inverted with the same tomographic approach by means of the Res2DInv software
 299 ([Loke and Barker, 1996](#)). Inverted resistivity data were similarly interpolated in order to allow a point
 300 by point comparison of all the resistivity maps obtained in terms of normalized differences (see later).

301

302 **4. RESULTS**

303 As far as raw data analysis is concerned, data from electric streamer measurements were, in general,
 304 slightly noisier (i.e. showing higher instrumental standard deviation and greater lateral variability) if
 305 compared to the ones obtained with traditional ERT. This was mainly due to local bad electrode-
 306 ground contacts, caused by the continuous moving of the system, and challenging initial field
 307 conditions at the moment of execution of the surveys (i.e. no rain for more than two months before
 308 the surveys and the presence of a gravel layer on the surface). Nevertheless, the high data coverage
 309 of the electric streamer allowed to perform the filtering operations avoiding no-data areas and the
 310 adopted irrigation system was effective in partially reducing the contact resistances even in very dry
 311 subsoil conditions.

312 Results of the acquisitions, in terms of apparent resistivity pseudo-sections, are reported in [Figure 4](#).



313
 314 **Figure 4 – Results of the ERT and electric streamer surveys in terms of apparent resistivity pseudo-**
 315 **sections along the studied embankments.**

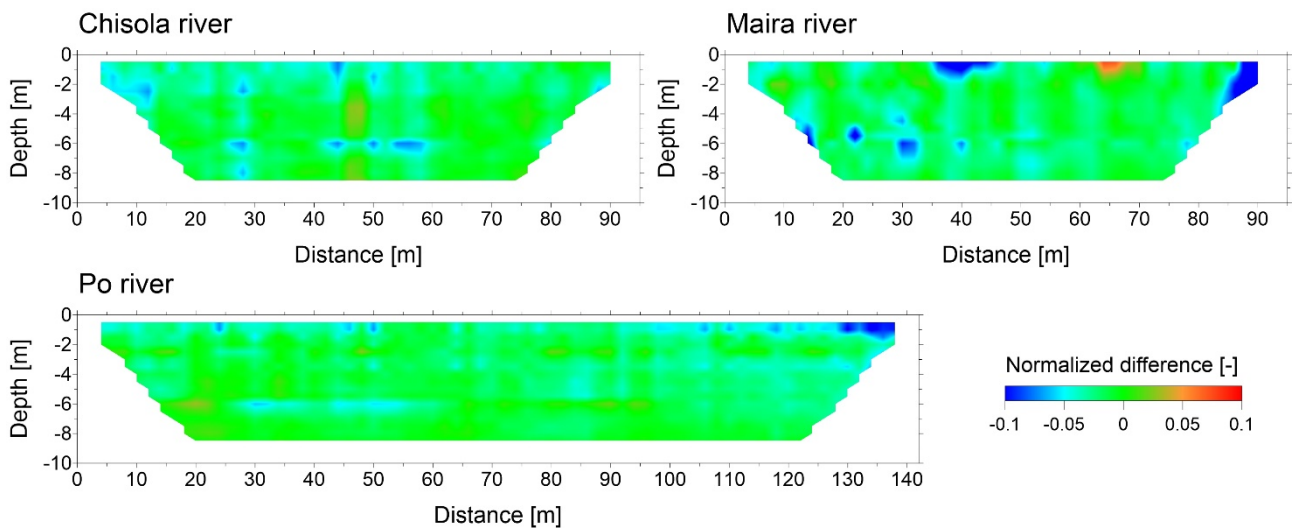
316 By analysing [Figure 4](#) it can be noted that the results of the two different surveys are highly
 317 comparable and that the main lateral and vertical variations observed along the ERT pseudo-sections
 318 are also recognized in the electric streamer pseudo-sections. Given the different data coverage of
 319 measurements ([Figure 3](#)) the main resistivity anomalies tend to be elongated in the vertical direction
 320 for ERT measurements, which has a reduced number of levels with depth, and in the horizontal
 321 direction for electric streamer measurements, due to the presence of multiple overlapping levels with

322 depth. Notwithstanding this different data coverage, the normalized differences between the two
 323 investigations, calculated for the superimposing portions of the surveys and reported in Figure 5,
 324 evidence that the data are in most of the situations within a $\pm 5\%$ difference, which is an indicator of
 325 the high comparability of acquired values. The normalized difference (ND) was calculated with the
 326 formula:

$$327 \quad ND = \frac{\rho_{aERT} - \rho_{aES}}{\rho_{aERT}} \quad (2)$$

328 where ρ_{aERT} is the apparent resistivity value obtained from ERT measurements and ρ_{aES} is the apparent
 329 resistivity value obtained from electric streamer measurements. Therefore, positive values of the
 330 normalized difference indicate zones where the electric streamer underestimate the apparent
 331 resistivity, negative values indicate the opposite.

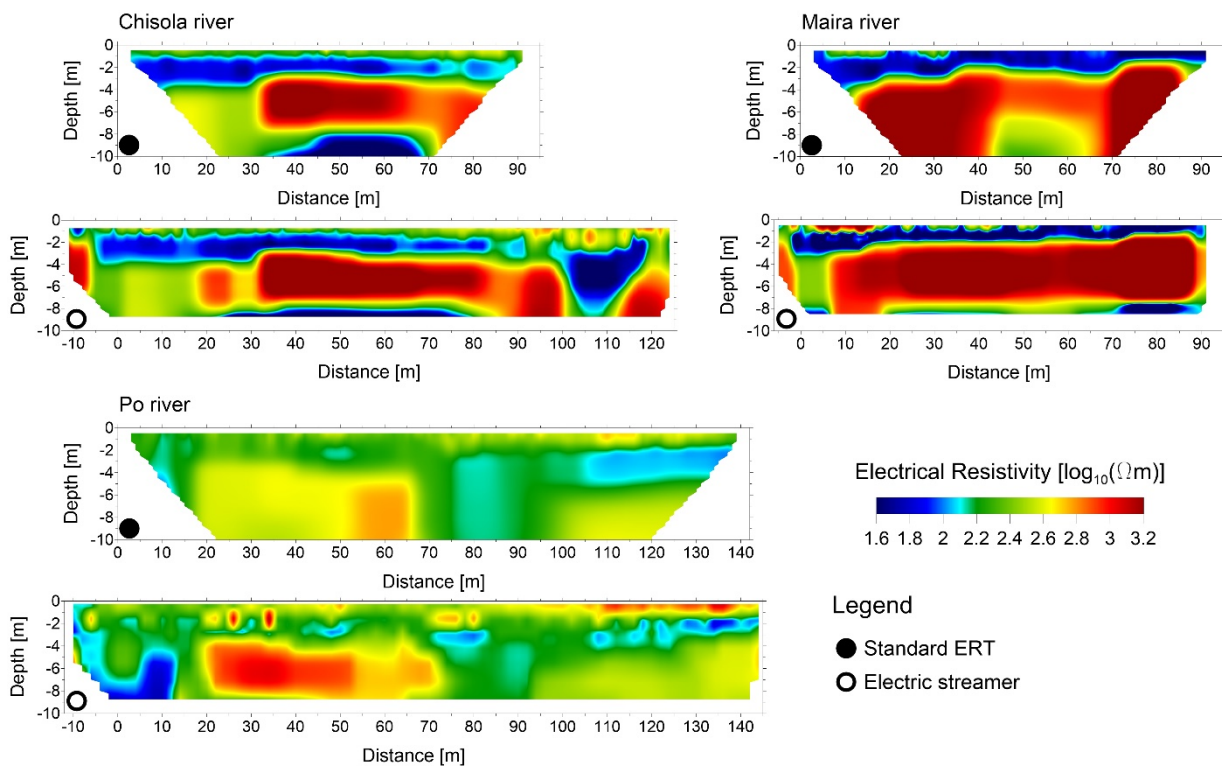
332 Most of the highest difference values, mostly negative, are located either along vertical or horizontal
 333 stripes. This striping effect is related to the different data coverage of the two surveys and evidence
 334 portions in which the data comparison could be more affected by interpolation than by differences in
 335 the measured values.



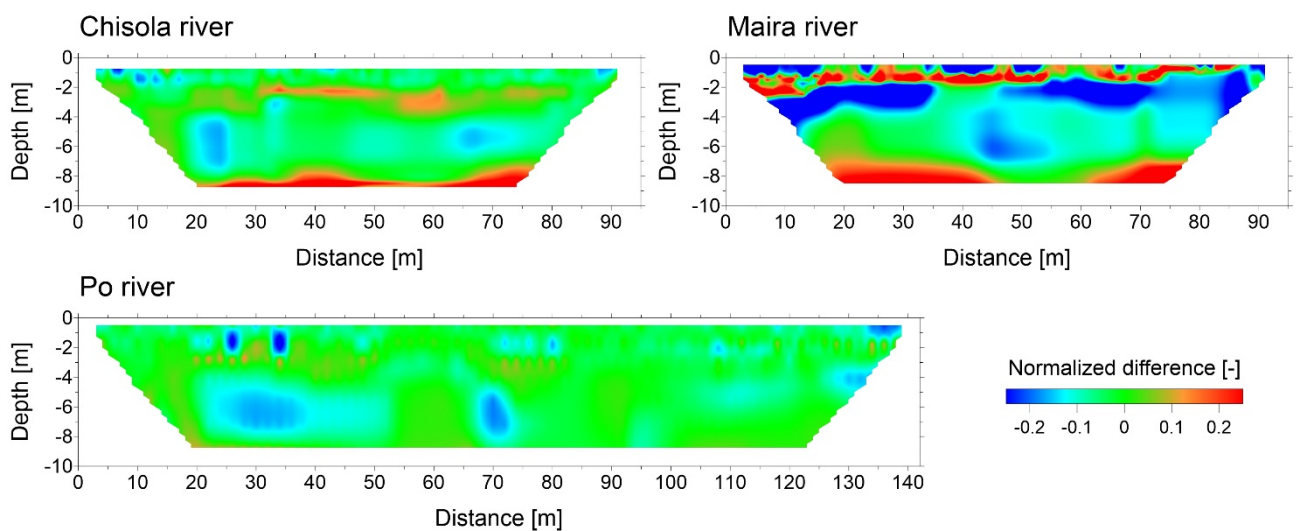
336
 337 **Figure 5 – Results of the ERT and electric streamer surveys in terms of normalized difference among**
 338 **the apparent resistivity pseudo sections of the two surveys along the studied embankments.**

339 The experimental apparent resistivity data were processed and inverted with the same tomographic
 340 approach by means of the Res2DInv software (Loke and Barker, 1996). For most of the inversions a
 341 reliable root means square error (rms) was obtained, on average around 5%. Electric streamer data
 342 showed in general relatively higher rms; this is however not an indicator of the lower quality of the
 343 inversions but of the increased amount of data to be fitted in each survey (as mentioned, more than
 344 three times than for ERT measurements).

345 The inverted resistivity sections are reported in Figure 6, in terms of resistivity values, and in Figure
 346 7 in terms of normalized differences, calculated for the superimposing portions of the surveys.
 347



348
 349 **Figure 6 – Results of the ERT and electric streamer surveys in terms of inverted resistivity sections along**
 350 **the studied embankments.**



351
 352 **Figure 7 – Results of the ERT and electric streamer surveys in terms of normalized difference among**
 353 **the inverted resistivity sections of the two surveys along the studied embankments.**

354

355 From these results it can be again observed that the main resistivity anomalies reported in the ERT
356 sections are also visible in the electric streamer sections. Particularly, in the aim of characterisation
357 and uniformity evaluation of the embankments the two data are comparable for the superimposing
358 portions. However, an increase in the normalized difference between ERT and electric streamer
359 results can be observed. Particularly at the Maira and Chisola river case studies, an increased
360 difference is noted for depths near the investigation depth limit of the electric streamer. Even if ERT
361 and electric streamer inverted models agree to indicate a decrease in resistivity values at those levels,
362 the electric streamer results tend to underestimate the resistivity values. This difference is related to
363 the different data coverage with depth of the ERT and electric streamer surveys (see [Figure 3](#)). When
364 the studied embankment is characterized by a silty, clayey lower resistivity layer, as it is the case for
365 the two mentioned cases, the current penetration of the electric streamer is reduced, given the reduced
366 electrodes spacings adopted. Therefore, in these situations a precautionary lower limit in the
367 investigation depth should be established. This penetration limit, as mentioned, will be even more
368 critical for capacitive coupled systems approaches.

369 Notwithstanding this limitation, most of the normalized differences in the resistivity values still fall
370 within a $\pm 5\%$ difference limit. Higher localized differences can be noted in the shallower portions of
371 the sections, most significative in the Maira case study. These may be related to stronger resistivity
372 contrasts between the embankment and the natural soil (as is the case for the Maira case study, [Figure](#)
373 [7](#)) or to localized anomalies evidenced by one of the two surveys only. Stronger contrasts and
374 localized anomalies involve indeed higher nonlinearity in the inversion problem (as is the case for
375 the Po case study, [Figure 7](#)). In these situations, inversion quality and the reconstruction of sharp
376 resistivity contrasts can be strongly influenced by measurements distribution. As mentioned above
377 the higher data coverage of the electric streamer potentially allow for a more accurate identification
378 of these localized contrasts.

379

380 **5. DISCUSSIONS**

381 The presented results showed that the new electric streamer developed for the study of river
382 embankments provided resistivity data highly comparable with the ones obtainable with standard
383 ERT acquisitions. Not only, in all the surveys the electric streamer data, in the adopted disposition
384 and measurement step, offered increased lateral coverage. As an example, along the Po river case
385 study, where the survey length of the two systems is the same, it can be observed how the electric
386 streamer is not affected by the lack of data points that characterize ERT, for the adopted electrodes
387 spacing, at the border of the surveyed section (see [Figure 4](#)). Moreover, the data coverage is also
388 increased within each section given that the number of electric streamer measurements is almost three

389 time than the one of ERT surveys (see [Table 1](#)). This result is clearly dependent on the adopted
390 streamer infrastructure and ERT survey setup. Ideally, the same data coverage could be obtained by
391 the two surveys, adopting similar measurements distributions and electrodes spacings. However,
392 performing this for ERT would require significant efforts on the field while the higher data coverage
393 can be obtained through streamer data with reduced survey time and efficiency.

394 The acquisition of electric streamer data is indeed a completely automatic process, once that the
395 streamer is deployed on the embankment surface. Each measurement step involves an acquisition
396 time of about 40 seconds, which could be eventually repeated when the contact resistances of
397 electrodes is still insufficiently reduced by the drip irrigation system. Deployment of the streamer can
398 be quantified around 15 to 20 minutes, depending on the number of people involved in the survey.
399 Conversely, acquisition of ERT data involves 45 to 90 min, depending on the measuring sequence
400 adopted, and deployment of ERT surveys is for sure more time consuming due to the necessity of
401 nailing the electrodes, connecting all the acquisition cables and watering the electrodes for ensuring
402 optimal galvanic contact. ERT survey time is directly proportional to the required spatial resolution,
403 making the electric streamer significantly more advantageous for the execution of fast surveys.

404 The better efficiency of the electric streamer is even higher for survey lengths longer than the ones
405 presented in the present paper, which were limited in the aim of a strict comparison of the results. For
406 increased survey lengths the acquisition of ERT data involve indeed the use of the roll-along
407 technique which requires to re-nail electrodes along successive portions of the line, reconnect and
408 move the cables, and highly increase the survey time. Performing longer surveys with the electric
409 streamer is instead only a matter of dragging the system for more time.

410 This increased efficiency potentially allows the streamer to be used also in situations where the speed
411 of the surveys is essential. This is the case, for example, in situations where a specific characterization
412 of embankments anomalies is required after, or during, large flood events. In these situations, a direct
413 imaging of the resistivity pseudo-section during surveys execution could be also foreseen. This is a
414 common approach adopted during the execution of resistivity surveys in water covered areas (e.g.
415 Sysmar, Iris instruments acquisition approach, [Colombero et al., 2014](#)). Its implementation with the
416 developed electric streamer is straightforward given that at each measurement step a new vertical
417 portion of the embankment is investigated and can be directly visualized on the pseudo-section. This
418 could allow a direct on site imaging of potentially dangerous anomalies. Moreover, a moving system
419 can serve different resolution requests, and the moving steps along the embankment structures can be
420 adjusted according to the desired target (i.e. larger moving steps for large scale characterization;
421 smaller moving steps for highly detailed surveys).

422 Partial limitations in the use of the newly developed electric streamer can be foreseen in some specific
423 conditions. The presence of a highly resistive shallow cover (i.e. presence of paved road or compacted
424 soil) along embankment summit could strongly limit the current injection capabilities
425 notwithstanding the used irrigation system. This situation could increase the survey time due to the
426 necessity to increase the irrigation time. This condition was partially encountered along the Maira
427 river embankment case study, not compromising however the overall quality of the measurements.
428 In similar conditions standard ERT surveys can easily overlap the shallow coverage thanks to the
429 electrode length. Also, the developed system is not designed for application along embankments with
430 relevant curves. The dragging of the system is indeed effective only along linear embankments
431 segments. This last limitation also affects standard ERT measurements and all problems to be solved
432 and represented in 2-D.

433 Further developments in the use of the electric streamer could include different types of geoelectrical
434 measurements rather than the only resistivity. Potentially, the streamer can be used for the execution
435 of both Induced Polarization (IP) and Self Potential (SP) measurements. As mentioned in the
436 introduction, IP measurements have greater potential in discriminating the effects of water content
437 and cation exchange capacity while SP measurements can be used to monitor self-potential signals
438 associated with seepage in embankments (e.g. [Soueid et al., 2020b](#)). However, the execution of both
439 these types of surveys would strongly increase the acquisition time, partially reducing the advantages
440 for which the developed electric streamer was designed.

441 Finally, an interesting development could be to combine the electric streamer with a seismic streamer,
442 merging the two systems for a joint acquisition of both geoelectrical and seismic data. The streamer
443 set-up and arrangement has been indeed designed in view of a future combination with seismic
444 sensors, to be then combined in a seismic-electric land-streamer. Conversely than for electric data
445 acquisitions, the technological development of seismic streamers is already well established in the
446 geophysical community. Several examples of high-quality seismic data collected with this approach
447 are available in literature (e.g. [Van Der Veen et al., 2001](#); [Pugin et al., 2004](#)). From the results
448 presented in this paper a combination of the newly developed electric streamer with a standard seismic
449 one can be therefore foreseen. The combined use of geoelectrical and seismic data can indeed provide
450 an even more effective geotechnical characterization of river embankments, as shown by several
451 research groups that are working on their integration (e.g. [Chen et al., 2006](#); [Takahashi et al., 2014](#);
452 [Goff et al., 2015](#)). Preliminary investigations performed with this approach ([Arato et al., 2020](#)) have
453 shown that the combination of the two streamers can increase even more the efficiency of the surveys
454 at strongly reduced acquisition times.

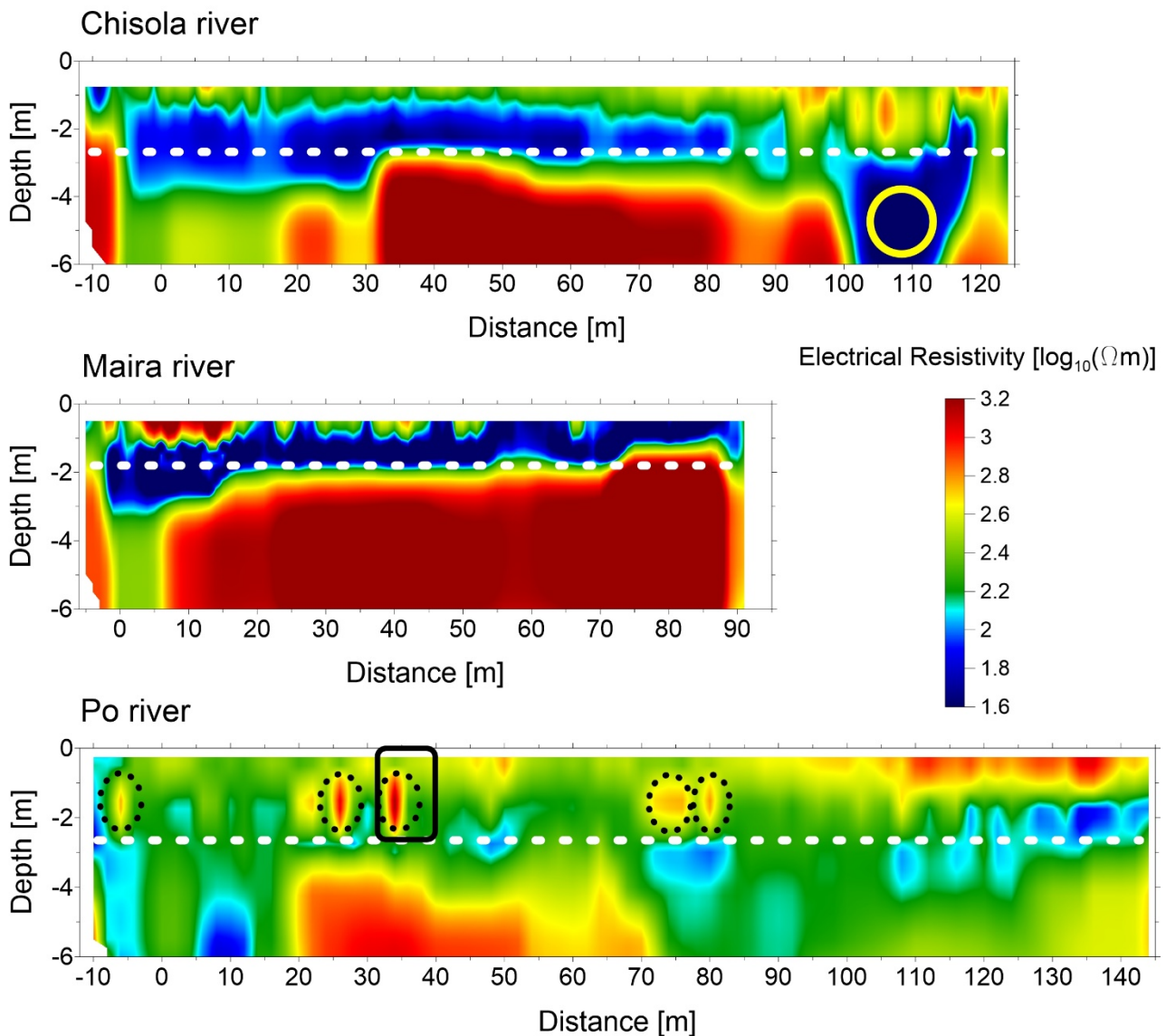
455 The comparison between electric streamer and ERT inverted resistivity sections has evidenced a
456 limited increase in the normalized difference among the two surveys. This increase is partially
457 expected given that the inversion process, due to its inherent non unicity, is highly conditioned by the
458 number of measurements and the data distribution. Therefore, the non-perfect correspondence of the
459 two results cannot be judged as a non-reliability of electric streamer data. Moreover, the anomalies
460 in the electric streamer resistivity sections, which does not have a correspondence in the ERT ones,
461 are related to good quality data (i.e. do not come from outlier data or measurement errors) and should
462 be linked to real and more intensely detected anomalies throughout the embankments.

463 Apart from the higher depth portions of the electric streamer sections, where probably the electric
464 streamer lacks in penetration and the resistivity models suffer from the different boundary assignment
465 by the inversion software, the results of the electric streamer surveys can be therefore considered
466 equally good as ERT surveys.

467 [Figure 8](#) reports the resulting resistivity models from the electric streamer surveys, focused in the
468 depth range between 0 to 6 m, that most properly characterizes the studied embankments. On these
469 sections, the known heights of the different embankments from the free surface is also reported (white
470 dashed line). Unfortunately, no data from other independent tests are available to better identify the
471 type/origin of evidenced anomalies, so discussions on these can be only speculative. However, the
472 focus here is more on the comparison between electric streamer and ERT results than on the origin
473 of the anomalies. In this respect, the presented case studies can be seen as examples of the application
474 of the newly developed measurement technique and its feasibility.

475 All case studies report a resistivity transition almost in correspondence of (on average about half a
476 meter lower) the known heights of the embankments. This is coherent with embankment construction
477 plans which included a shallow removal of topsoil. In the Maira and Chisola case studies the
478 resistivity transition from the embankment to the natural soil is sharper. This is related to the mostly
479 silty and clayey nature of these two embankments, having lower resistivities with respect to the
480 natural alluvial soils of the plain, which are coarser instead. Along these embankments a shallow
481 more resistive coverage is also evidenced, due to the presence of a thin gravel layer put in place to
482 pave the road on the embankment summit and also to the presence of a poorly saturated layer on top
483 of the embankments.

484



485
 486 **Figure 8 – Results of the electric streamer surveys in terms of inverted resistivity sections along the**
 487 **studied embankments with evidence of their attended depth (white dashed lines) and anomalies: low**
 488 **resistivity anomaly along the Chisola river embankment (yellow circle); known badger burrow portion**
 489 **(black square) and potentially void borrows (black dashed ellipses) along the Po river embankment.**
 490

491 The newly constructed Maira river embankment appears to be quite uniform, in terms of resistivity
 492 values, in the investigated length. This indicates a uniform and effective constructing procedure.
 493 Minor variations in the depth of the embankment are evidenced probably related to different soil
 494 removal in the bottom parts. A zone with a shallow high resistivity anomaly is also observable along
 495 this embankment between 0 and 20 m. A similar increase in resistivity can be also partially seen in
 496 the ERT results (Figure 6). This may be related to an increased thickness of the gravel layer on the
 497 surface. No evidences related to the lateral landslips along the slopes are however reported.

498 Along the Chisola river embankment a significant low resistivity anomaly (yellow circle in [Figure 8](#))
499 is evidenced. This could be related to a potential seepage hazard zone. The reduced resistivity of this
500 area cannot be indeed correlated with lateral soil variations, which are quite uniform in the plain, but
501 are most probably related to an increase in the water content of the ground.
502 Partially different results are obtained along the Po river case study. Here, the transition from the
503 embankment material to the natural soil appears to be smoother, given its more dated construction,
504 and inner resistivity heterogeneities can be related to different conferred materials, probably exploited
505 from surrounding sand/gravel caves or directly from fine river deposits. The AIPO alerted about the
506 presence of a known badger burrow in the portion from 32 to 40 m (black square in [Figure 8](#)). Within
507 this area a local high resistivity anomaly, potentially correlated to the void burrow, is indeed notable
508 (black dashed ellipse). Similar anomalies are also noted in other locations along the investigated
509 portion (with no visual or direct external appearance) and can be suggested as probable attention
510 zones. Their position near the embankment bottom is indeed compatible with animal activity. The
511 effectiveness in the indication of these anomalies, which are less clear from the ERT results (see
512 [Figure 6](#)), is a further demonstration of the increased data coverage of the developed streamer and the
513 high resolution it can offer in the characterization.

514

515 **6. CONCLUSIONS**

516 A new electric streamer was developed within this work to allow for the execution of fast ERT (but
517 potentially any geoelectric) surveys in motion along river embankments. The new system was
518 developed to guarantee an investigation depth covering the whole embankment body and foundation
519 soil, overcoming current limitations of available similar instrumentation usually adopted for
520 geoelectrical surveys in motion. The technical solutions adopted for its construction (electrodes
521 design and irrigation system) allowed the acquisition of reliable resistivity data, alternative to
522 electrode nailing into the ground.

523 The results presented and commented in the paper shown that the newly developed electric streamer
524 provided data which are strictly comparable to standard ERT data acquired as benchmarks. The
525 adopted streamer arrangement and measurement step showed advantages in reducing survey time and
526 increasing the system efficiency. Its application as a fast screening tool can be foreseen near main
527 flood events affecting relevant portions of river embankments in different contexts. The streamer
528 data, with the current electrode disposition, were acquired over multiple overlapping levels, offering
529 an increased lateral and vertical coverage with respect to standard ERT surveys and entailing on a

530 more accurate definition of localized anomalies related to animal borrows within one of the case
531 studies.

532 The resulting resistivity models allowed to characterize peculiar anomalies along the studied
533 embankments, even though the nature and properties of these anomalies should be better studied with
534 the use of local geotechnical investigations to have a more specific knowledge on the state of life of
535 the embankments. With this respect, a natural development of the instrumentation can be foreseen
536 with the implementation of rapid tools for direct in-situ mapping of apparent resistivity pseudo-
537 sections resulting from the surveys. This implementation is straightforward, and the apparent
538 resistivity pseudo-section can be plotted and directly visualized by adding new data at each
539 measurement step along the streamer profile. This will allow a direct imaging of anomalous points
540 and a fast identification of the zones of the embankment where integrative localized tests or specific
541 intervention are necessary.

542 Further studies, already planned and partially executed, include the application of the new electric
543 streamer for embankment depths greater than the ones presented in this paper and along longer survey
544 profiles. Moreover, the combination of the present electric streamer with a standard seismic streamer
545 will allow for joint resistivity and seismic surveys, profiting by the contemporary acquisition of
546 electric and seismic data at each measurement step and further optimizing survey time. The combined
547 acquisition of multiple geophysical parameters could improve the knowledge on the performance of
548 river embankments and provide input data for specific correlations and modelling with relevant
549 hydraulic and geotechnical parameters.

550 **ACKNOWLEDGMENTS**

551 This work has been funded by FINPIEMONTE within the POR FESR 14/20 "Poli di Innovazione -
552 Agenda Strategica di Ricerca 2016 - Linea B" call for the project Mon.A.L.I.S.A. (313-67). Authors
553 thank Daniele Negri for helping during acquisition surveys and are indebted with the Torino-
554 Moncalieri AIPO division, and related personnel, for access permissions and for sharing information
555 about the studied embankments.

556 **REFERENCES**

- 557 Abdulsamad, F., Revil, A., Soueid Ahmed, A., Coperey, A., Karaoulis, M., Nicaise, S., Peyras, L.,
558 2019. Induced polarization tomography applied to the detection and the monitoring of leaks in
559 embankments. *Eng. Geol.* 254, 89–101. <https://doi.org/10.1016/j.enggeo.2019.04.001>
- 560 Al-Fares, W., 2014. Application of electrical resistivity tomography technique for characterizing
561 leakage problem in Abu Baara earth dam, Syria. *Int. J. Geophys.* 2014.
562 <https://doi.org/10.1155/2014/368128>
- 563 An, N., Tang, C.S., Cheng, Q., Wang, D.Y., Shi, B., 2020. Application of electrical resistivity
564 method in the characterization of 2D desiccation cracking process of clayey soil. *Eng. Geol.*
565 265. <https://doi.org/10.1016/j.enggeo.2019.105416>
- 566 Arato, A., Naldi M., Vai, L., Chiappone, A., Vagnon, F., Comina, C., 2020. Towards a Seismo-Electric land
567 streamer. In proceedings of the 6th International Conference on Geotechnical and Geophysical Site
568 Characterization, 7-11 September 2020, Budapest.
- 569 Arosio, D., Munda, S., Tresoldi, G., Papini, M., Longoni, L., Zanzi, L., 2017. A customized
570 resistivity system for monitoring saturation and seepage in earthen levees: Installation and
571 validation. *Open Geosci.* 9, 457–467. <https://doi.org/10.1515/geo-2017-0035>
- 572 Barker, R.D., 1989. Depth of investigation of collinear symmetrical four-electrode arrays,
573 *Geophysics*, 54, 1031-1037.
- 574 Binley, A., Slater, L.D., Fukes, M., Cassiani G., 2005. Relationship between spectral induced
575 polarization and hydraulic properties of saturated and unsaturated sandstone, *Water Resour.*
576 *Res.*, 2005, vol. 41 12 doi:10.1029/2005WR004202
- 577 Borgatti, L., Forte, E., Mocnik, A., Zambrini, R., Cervi, F., Martinucci, D., Pellegrini, F., Pillon, S.,
578 Prizzon, A., Zamariolo, A., 2017. Detection and characterization of animal burrows within
579 river embankments by means of coupled remote sensing and geophysical techniques: Lessons
580 from River Panaro (northern Italy). *Eng. Geol.* 226, 277–289.
581 <https://doi.org/10.1016/j.enggeo.2017.06.017>
- 582 Borner, F.D., Schopper, J.R., Weller, A.. 1996. Evaluation of transport and storage properties in the
583 soil and groundwater zone from induced polarization measurements, *Geophys. Prospect.*,
584 1996, vol. 44 4(pg. 583-601)

- 585 Busato, L., Boaga, J., Peruzzo, L., Himi, M., Cola, S., Bersan, S., Cassiani, G., 2016. Combined
586 geophysical surveys for the characterization of a reconstructed river embankment. *Eng. Geol.*
587 211, 74–84. <https://doi.org/10.1016/j.enggeo.2016.06.023>
- 588 Camarero, P.L., Moreira, C.A., Pereira, H.G., 2019. Analysis of the Physical Integrity of Earth
589 Dams from Electrical Resistivity Tomography (ERT) in Brazil. *Pure Appl. Geophys.* 176,
590 5363–5375. <https://doi.org/10.1007/s00024-019-02271-8>
- 591 Cardarelli, E., Cercato, M., De Donno, G., 2014. Characterization of an earth-filled dam through the
592 combined use of electrical resistivity tomography, P- and SH-wave seismic tomography and
593 surface wave data. *J. Appl. Geophys.* 106, 87–95.
594 <https://doi.org/10.1016/j.jappgeo.2014.04.007>
- 595 Chen, C., Liu, J., Xia, J., Li, Z., 2006. Integrated geophysical techniques in detecting hidden
596 dangers in river embankments. *J. Environ. Eng. Geophys.* 11, 83–94.
597 <https://doi.org/10.2113/JEEG11.2.83>
- 598 Cho, I.K., Yeom, J.Y., 2007. Crossline resistivity tomography for the delineation of anomalous
599 seepage pathways in an embankment dam. *Geophysics* 72. <https://doi.org/10.1190/1.2435200>
- 600 Colombero, C., Comina, C., Gianotti, F., Sambuelli, L., 2014. Waterborne and on-land electrical
601 surveys to suggest the geological evolution of a glacial lake in NW Italy. *J. Appl. Geophys.*
602 105, 191–202. <https://doi.org/10.1016/j.jappgeo.2014.03.020>
- 603 Dabas, M., 2008. Theory and practice of the new fast electrical imaging system ARP©, in: *Seeing*
604 *the Unseen: Geophysics and Landscape Archaeology*. pp. 105–126.
605 <https://doi.org/10.1201/9780203889558.ch5>
- 606 Edwards L.S., 1977. A modified pseudosection for resistivity and induced-polarization,
607 *Geophysics*, 42, 1020-1036.
- 608 Goff, D.S., Lorenzo, J.M., Hayashi, K., 2015. Resistivity and shear wave velocity as a predictive
609 tool of sediment type in coastal levee foundation soils, in: *28th Symposium on the Application*
610 *of Geophysics to Engineering and Environmental Problems 2015, SAGEEP 2015*. pp. 145–
611 154.
- 612 Jodry, C., Palma Lopes, S., Fargier, Y., Sanchez, M., Côte, P., 2019. 2D-ERT monitoring of soil
613 moisture seasonal behaviour in a river levee: A case study. *J. Appl. Geophys.* 167, 140–151.
614 <https://doi.org/10.1016/j.jappgeo.2019.05.008>
- 615 Jones, G., Sentenac, P., Zielinski, M., 2014. Desiccation cracking detection using 2-D and 3-D
616 electrical resistivity tomography: Validation on a flood embankment. *J. Appl. Geophys.* 106,
617 196–211. <https://doi.org/10.1016/j.jappgeo.2014.04.018>
- 618 Jougnot, D., Ghorbani, A., Revil, A., Leroy, P., Cosenza, P., 2010. Spectral induced polarization of
619 partially saturated clay-rocks: A mechanistic approach. *Geophys. J. Int.* 180, 210–224.
620 <https://doi.org/10.1111/j.1365-246X.2009.04426.x>
- 621 Kuras, O., Meldrum, P.I., Beamish, D., Ogilvy, R.D., Lala, D., 2007. Capacitive resistivity imaging
622 with towed arrays. *J. Environ. Eng. Geophys.* 12, 267–279.
623 <https://doi.org/10.2113/JEEG12.3.267>

- 624 Lee, S.K., Cho, S.J, Song, Y., Chung, S.H. 2002. Capacitively-coupled Resistivity Method -
625 Applicability and Limitation. *Geophys. and Geophysic. Explor.* 5(1), 23-32. Lee, B., Oh, S., Yi,
626 M.J., 2020. Mapping of leakage paths in damaged embankment using modified resistivity
627 array method. *Eng. Geol.* 266. <https://doi.org/10.1016/j.enggeo.2019.105469>
- 628 Loke, M.H., Barker, R.D., 1996. Rapid least-squares inversion of apparent resistivity
629 pseudosections by a quasi-Newton method. *Geophys. Prospect.* 44, 131–152.
630 <https://doi.org/10.1111/j.1365-2478.1996.tb00142.x>
- 631 Minsley, B.J., Burton, B.L., Ikard, S., Powers, M.H., 2011. Hydrogeophysical investigations at
632 hidden Dam, Raymond, California. *J. Environ. Eng. Geophys.* 16, 145–164.
633 <https://doi.org/10.2113/JEEG16.4.145>
- 634 Panthulu, T. V., Krishnaiah, C., Shirke, J.M., 2001. Detection of seepage paths in earth dams using
635 self-potential and electrical resistivity methods. *Eng. Geol.* 59, 281–295.
636 [https://doi.org/10.1016/S0013-7952\(00\)00082-X](https://doi.org/10.1016/S0013-7952(00)00082-X)
- 637 Pugin, A.J.M., Larson, T.H., Sargent, S.L., McBride, J.H., Bexfield, C.E., 2004. Near-surface
638 mapping using SH-wave and P-wave seismic land-streamer data acquisition in Illinois, U.S.
639 *Lead. Edge* 23, 677–682. <https://doi.org/10.1190/1.1776740>
- 640 Sjö Dahl, P., Dahlin, T., Zhou, B., 2006. 2.5D resistivity modeling of embankment dams to assess
641 influence from geometry and material properties. *Geophysics* 71.
642 <https://doi.org/10.1190/1.2198217>
- 643 Sørensen, K., 1996. Pulled array continuous electrical profiling. *First Break* 14, 85–90.
644 <https://doi.org/10.4133/1.2922124>
- 645 Soueid Ahmed, A., Revil, A., Abdulsamad, F., Steck, B., Vergnialt, C., Guihard, V., 2020a.
646 Induced polarization as a tool to non-intrusively characterize embankment hydraulic
647 properties. *Eng. Geol.* 271. <https://doi.org/10.1016/j.enggeo.2020.105604>
- 648 Soueid Ahmed, A., Revil, A., Bolève, A., Steck, B., Vergnialt, C., Courivaud, J.R., Jougnot, D.,
649 Abbas, M., 2020b. Determination of the permeability of seepage flow paths in dams from self-
650 potential measurements. *Eng. Geol.* 268. <https://doi.org/10.1016/j.enggeo.2020.105514>
- 651 Takahashi, T., Aizawa, T., Murata, K., Nishio, H., Consultants, S., Matsuoka, T., 2014. Soil
652 permeability profiling on a river embankment using integrated geophysical data, in: *Society of*
653 *Exploration Geophysicists International Exposition and 84th Annual Meeting SEG 2014.* pp.
654 4534–4538. <https://doi.org/10.1190/segam2014-0620.1>
- 655 Tresoldi, G., Arosio, D., Hojat, A., Longoni, L., Papini, M., Zanzi, L., 2019. Long-term
656 hydrogeophysical monitoring of the internal conditions of river levees. *Eng. Geol.* 259.
657 <https://doi.org/10.1016/j.enggeo.2019.05.016>
- 658 Van Der Veen, M., Spitzer, R., Green, A.G., Wild, P., 2001. Design and application of towed land-
659 streamer system for cost-effective 2-D and pseudo-3-D shallow seismic data acquisition.
660 *Geophysics* 66, 482–500. <https://doi.org/10.1190/1.1444939>

661